Nonlinear dissipative dynamics of a two-component atomic condensate coupling with a continuum*

Zhong Hong-Hua(钟宏华)[a)b)†], Xie Qiong-Tao(谢琼涛)[b)c)], Xu Jun(徐 军)[b)], Hai Wen-Hua(海文华)[c)], and Li Chao-Hong(李朝红)[b)]

[a)] *Department of Physics, Jishou University, Jishou* 416000, *China*

[b)] *State Key Laboratory of Optoelectronic Materials and Technologies, School of Physics and Engineering, Sun Yat-Sen University, Guangzhou* 510275, *China*

[c)] *Department of Physics and Key Laboratory of Low-Dimensional Quantum Structure and Quantum Control of Ministry of Education, Hunan Normal University, Changsha* 410081, *China*

(Received 27 April 2013; revised manuscript received 24 June 2013; published online 20 December 2013)

We investigate the nonlinear dissipative coherence bifurcation and population dynamics of a two-component atomic Bose–Einstein condensate coupling with a continuum. The coupling between the two-component condensates and the continuum brings effective dissipations to the two-component condensates. The steady states and the coherence bifurcation depend on both dissipation and the nonlinear interaction between condensed atoms. The coherence among condensed atoms may be even enhanced by the effective dissipations. The combination of dissipation and nonlinearity allows one to control the switching between different self-trapped states or the switching between a self-trapped state and a non-self-trapped state.

Keywords: Bose–Einstein condensate, nonlinear dynamics, quantum tunneling, open quantum system

PACS: 03.75.Kk, 03.75.Gg, 03.75.Lm, 05.30.Jp **DOI:** 10.1088/1674-1056/23/2/020314

1. Introduction

Since the experimental realization of the two-component condensates, such as Bose–Einstein condensates (BECs) of ^{87}Rb in two different hyperfine levels,[1–6] the dynamical features of two-component condensates have been widely investigated in recent years. Within the mean-field description, several macroscopic quantum behaviors and interesting dynamical properties[7–23] have been explored. Within the quantum-field description, several many-body quantum phenomena,[24–38] such as quantum self-trapping[26,27] and spontaneous symmetry breaking,[38] have been predicted. Some of these dynamical properties have also been observed in experiments.[1,39]

In real experiments, due to the atomic loss induced by inelastic collisions and the coexistence of condensed and non-condensed atoms,[40–42] the atomic condensates are not absolutely closed systems. The dissipative processes can be effectively described by non-Hermitian (NH) Hamiltonians.[43–47] The dissipation-induced effects in an NH Bose–Hubbard dimer with a complex on-site energy[48–51] or a complex coupling term[52] have been studied extensively. If a system has an intrinsic mechanism balancing the dissipations, the dissipation can lead to a constructive effect, such as the enhanced self-trapping[49,50] and the inhibited losses of atoms.[53] Moreover, the dissipation-induced coherence in an open two-mode BEC system have been studied by the master equation method.[54–56]

In single-particle systems, the interaction between a two-state model and a continuum is a paradigm to understand the quasi-stationary states.[57,58] Up to now, there has been no study of the coupling between a many-body two-state system with continuum. The experimental realization of two-component BEC provides a new possibility for exploring many-body quantum phenomena of atoms coupled with continuum, such as many-body coherence, dissipative dynamics, and population transition. Therefore, the study of two-component condensates coupling with continua will provide a benchmark for understanding dissipative many-body quantum systems.

In this article, we investigate the many-body quantum coherence and population dynamics in a two-component condensate coupled with a continuum. Our system can be described by an effective NH Bose–Hubbard dimer with complex diagonal and off-diagonal elements, which are induced by the continuum. In the mean-field theory, the system obeys a two-mode NH Gross–Pitaevskii Hamiltonian, in which the nonlinear terms describe the atom–atom interactions. We find that the combination of dissipation and nonlinearity may induce different steady states and modify the coherence bifurcation. By tuning the nonlinearity and dissipation strength, it is

*Project supported by the National Basic Research and Development Program of China (Grant No. 2012CB821305), the National Natural Science Foundation of China (Grant Nos. 11075223, 11147021, 10905019, and 11175064), the Program for Changjiang Scholars and Innovative Research Team in University (Grant No. IRT0964), the Natural Science Foundation of Hunan Province, China (Grant No. 12JJ4010), the Program for New Century Excellent Talents in University (Grant No. NCET-10-0850), and the Ph. D. Programs Foundation of the Ministry of Education of China (Grant No. 20120171110022).

†Corresponding author. E-mail: hhzhong115@163.com

© 2014 Chinese Physical Society and IOP Publishing Ltd

possible to observe the coherence enhancement. Particularly, different relative dissipation strengths between two hyperfine levels will drive the two-component condensates into different stable states. In the time evolution, the system can jump from one stable state to another stable state and the switching time depends on the nonlinearity strength. The combination of dissipation and nonlinearity can be used to manipulate the steady behaviors; such as, controlling the transition between two self-trapping states or between a self-trapped state and a non-self-trapped state. Therefore, our results provide an alternative route for manipulating the many-body coherence and population dynamics by controlling and utilizing dissipation and nonlinearity.

The structure of this article is as follows. In Section 2, we give the NH Hamiltonian and the equations of motion. In Section 3, we analyze that how dissipation and nonlinearity affect the bifurcation of coherence. In Section 4, we show various nonlinear dissipative dynamics under different conditions. In the last section, we briefly summarize our results.

2. NH two-mode Bose–Hubbard model

We consider the interaction between a two-component condensate, whose atoms occupy two different hyperfine levels, and a continuum. The two hyperfine levels are coupled by a Raman laser, and interact with a common continuum by external fields.[57,59,60] With the well-known single-mode approximation, and by eliminating atoms in continuum,[57,58] the system obeys the Hamiltonian

$$\begin{aligned}\hat{H} &= \left(\Omega - \mathrm{i}\sqrt{\Gamma_1\Gamma_2}/2\right)\left(b_1^\dagger b_2 + b_2^\dagger b_1\right) + U_{12} b_1^\dagger b_2^\dagger b_2 b_1 \\ &\quad + \sum_{j=1,2}\left[\left(\varepsilon_j - \mathrm{i}\frac{\Gamma_j}{2}\right) b_j^\dagger b_j + \frac{U_{jj}}{2} b_j^\dagger b_j^\dagger b_j b_j\right]. \end{aligned} \tag{1}$$

Here $b_j^\dagger$ (b_j) are the bosonic creation (annihilation) operators for atoms occupying the j-th hyperfine level. In the complex coupling term, $\Omega - \mathrm{i}\sqrt{\Gamma_1\Gamma_2}/2$, Ω denotes the direct coupling between the two hyperfine levels and $\mathrm{i}\sqrt{\Gamma_1\Gamma_2}/2$ describes the effective coupling between them via the continuum.[57,58] The inter-component interaction U_{jj} and the intra-component interaction U_{12} can be controlled by adjusting the atomic s-wave scattering lengths via Feshbach resonance techniques. In the complex energies, $\varepsilon_j - \mathrm{i}\Gamma_j/2$, the imaginary parts Γ_j denote dissipation rates for atoms in the j-th hyperfine level due to the interaction with the continuum.[57,58] For the case of $\Gamma_2 = 0$, the system (1) is just the model studied in Refs. [49] and [50]. For the case of no atom–atom interaction, $U_{jj} = U_{12} = 0$, the system (1) is reduced to the single-atom system.[57,58] To simplify, we set $\hbar = 1$ and adopt Ω as a unit to rescale the other parameters ε_j, Γ_j, U_{12}, and U_{jj}.

To investigate the dynamics of the system (1) in the Bloch representation, we introduce the angular momentum operators,

$$\begin{aligned} L_x &= \frac{1}{2}(b_1^\dagger b_2 + b_1 b_2^\dagger), \\ L_y &= \frac{1}{2i}(b_2^\dagger b_1 - b_1^\dagger b_2), \\ L_z &= \frac{1}{2}(b_2^\dagger b_2 - b_1^\dagger b_1), \end{aligned} \tag{2}$$

whose Casimir invariant is $L^2 = (N/2)(N/2+1)$. Here $N = b_1^\dagger b_1 + b_2^\dagger b_2$ is the total number operator. With these angular momentum operators, by omitting the real constant terms $O(N)$ and $O(N^2)$,[49,50] the Hamiltonian (1) can be written as

$$\hat{H} = 2(\Omega - \mathrm{i}\Lambda)L_x + GL_z^2 + (\delta - \mathrm{i}\gamma)L_z - \mathrm{i}\Upsilon N, \tag{3}$$

where $\Lambda = \sqrt{\Gamma_1\Gamma_2}/2$,

$$\begin{aligned} G &= (U_{11} + U_{22} - 2U_{12})/2, \\ \delta &= \varepsilon_2 - \varepsilon_1 + (U_{22} - U_{11})(N-1)/2, \end{aligned}$$

$\gamma = (\Gamma_2 - \Gamma_1)/2$, and $\Upsilon = (\Gamma_1 + \Gamma_2)/4$.

To investigate the mean-field dynamics, introducing the $SU(2)$ coherent states

$$|x_1, x_2\rangle = \frac{1}{\sqrt{N!}}(x_1 b_1^\dagger + x_2 b_2^\dagger)^N |0,0\rangle, \tag{4}$$

with two complex coefficients x_j, the mean-field Bloch vectors $s_k = \langle L_k\rangle/N$, $k = x, y, z$, read as

$$\begin{aligned} s_x &= \frac{\langle x_1, x_2|L_x|x_1, x_2\rangle}{\langle x_1, x_2|x_1, x_2\rangle N} = \frac{(x_1^* x_2 + x_1 x_2^*)}{2n}, \\ s_y &= \frac{\langle x_1, x_2|L_y|x_1, x_2\rangle}{\langle x_1, x_2|x_1, x_2\rangle N} = \frac{(x_2^* x_1 - x_1^* x_2)}{2in}, \\ s_z &= \frac{\langle x_1, x_2|L_z|x_1, x_2\rangle}{\langle x_1, x_2|x_1, x_2\rangle N} = \frac{(x_2^* x_2 - x_1^* x_1)}{2n}. \end{aligned} \tag{5}$$

Here, $n = |x_1|^2 + |x_2|^2$ is the norm. By using the method developed in Refs. [49] and [50], the equations of motion for the Bloch vector are given as

$$\begin{aligned} \dot{s_x} &= -(\delta + 2Cs_z)s_y + 2\gamma s_z s_x - \Lambda(1 - 4s_x^2), \\ \dot{s_y} &= (\delta + 2Cs_z)s_x - 2\Omega s_z + 4\Lambda s_x s_y + 2\gamma s_z s_y, \\ \dot{s_z} &= 2\Omega s_y + 4\Lambda s_z s_x - \gamma(1 - 4s_z^2)/2. \end{aligned} \tag{6}$$

To obtain these equation, we have taken the semiclassical limit $N \to \infty$ with the mean-field interaction strength $C = NG$ kept unchanged. Therefore, $s^2 = s_x^2 + s_y^2 + s_z^2 = 1/4$ is a constant and the dynamics are regular and confined onto the Bloch sphere. However, the total probability n decays as

$$\dot{n} = -2(2\Lambda s_x + \gamma s_z + \Upsilon)n. \tag{7}$$

The Bloch equation (6) can also be equivalent to a generalized NH nonlinear Schrödinger equation. Introducing the unnormalized complex numbers ψ_j, which are associated with the coefficients x_j of the many-particle coherent

state,[49] the Bloch equation (6) corresponds to the NH nonlinear Schrödinger equation

$$\begin{aligned} & \mathrm{i}\frac{\mathrm{d}}{\mathrm{d}t}\begin{pmatrix}\psi_1\\ \psi_2\end{pmatrix} \\ &= \begin{pmatrix} -\delta/2 - C\kappa - \mathrm{i}(\Upsilon-\gamma/2) & \Omega - \mathrm{i}\Lambda \\ \Omega - \mathrm{i}\Lambda & \delta/2 + C\kappa - \mathrm{i}(\Upsilon+\gamma/2)\end{pmatrix} \\ &\times \begin{pmatrix}\psi_1\\ \psi_2\end{pmatrix}, \end{aligned} \tag{8}$$

with $\kappa = (|\psi_2|^2 - |\psi_1|^2)/(|\psi_1|^2 + |\psi_2|^2)$. Similar NH nonlinear Schrödinger equations have recently been proposed to describe open atomic BECs[49,50,61] and double-channel waveguide with gain and loss.[62,63]

3. Coherence bifurcation under dissipation and nonlinearity

In this section, we investigate the combined effects of the dissipation and nonlinearity on the phase coherence between two modes. Here we use the contrast in interference experiments to measure the phase coherence. The contrast is defined as[54–56]

$$\alpha = \frac{2\,|\,\langle b_1^\dagger b_2\rangle\,|}{\langle b_1^\dagger b_1 + b_2^\dagger b_2\rangle} = \sqrt{s_x^2 + s_y^2}. \tag{9}$$

In this work, we mainly focus on the coherence of the steady states (the fixed points of the equations of motion). These steady states can be calculated numerically via Newton flow method from $\dot{s} = 0$.[64] For the case of $\delta = 0$, we have

$$\begin{aligned} s_x^0 &= \frac{s_z^0[Q(2\Lambda C s_z^0 - \gamma\Omega) + 4\Omega(\Lambda^2+\Omega^2)]}{2[Q\Lambda\Omega + 2Cs_z^0(4\Lambda^2(s_z^0)^2 + \Omega^2)]}, \\ s_y^0 &= \frac{Q - 8\Lambda s_z^0 s_x^0}{4\Omega}, \end{aligned} \tag{10}$$

where $Q = \gamma[1 - 4(s_z^0)^2]$ and s_k^0 denote the corresponding fixed points. By using Eq. (10) and the normalization condition $s^2 = (s_x^0)^2 + (s_y^0)^2 + (s_z^0)^2 = 1/4$, we determine the values of s_z^0 and then s_x^0 and s_y^0 from Eq. (10). A key issue is the stability of the fixed points. To do this, we linearize Eq. (6) around the fixed points by substituting

$$s_x = s_x^0 + \Delta s_x, \quad s_y = s_y^0 + \Delta s_y, \quad s_z = s_z^0 + \Delta s_z, \tag{11}$$

with a small deviation $(\Delta s_x,\ \Delta s_y,\ \Delta s_z)$ into Eq. (6); thereby, one can obtain a linearized equation for this small deviation[54,55,65,66]

$$\frac{\mathrm{d}}{\mathrm{d}t}\begin{pmatrix}\Delta s_x\\ \Delta s_y\\ \Delta s_z\end{pmatrix} = M\begin{pmatrix}\Delta s_x\\ \Delta s_y\\ \Delta s_z\end{pmatrix}, \tag{12}$$

with the coefficient matrix

$$M = \begin{pmatrix} 2\gamma s_z^0 + 8\Lambda s_x^0 & -2Cs_z^0 & 2\gamma s_x^0 - 2Cs_y^0 \\ 2Cs_z^0 + 4\Lambda s_y^0 & 4\Lambda s_x^0 + 2\gamma s_z^0 & 2Cs_x^0 - 2\Omega + 2\gamma s_y^0 \\ 4\Lambda s_z^0 & 2\Omega & 4\Lambda s_x^0 + 4\gamma s_z^0 \end{pmatrix}. \tag{13}$$

The fixed points are linearly stable if, and only if, there are no eigenvalues with a positive real part for the coefficient matrix M. The eigenvalues of the coefficient matrix can be obtained numerically.

We show our numerical results for the steady contrast α in Fig. 1. The dependence of α on the relative dissipation strength γ and the imaginary coupling strength Λ are shown for two different cases: (a) the linear case $C = 0$ and (b) the nonlinear case $C = 1$. In Figs. 1(c) and 1(d), we plot the sections of Figs. 1(a) and 1(b) for $\gamma = 1$ and $\Lambda = 1$, respectively. The other parameters are given as $\Omega = 1$ and $\delta = 0$. The numerical results indicate that there exist two fixed points for the nonlinear case of $C = 1$ while there only exists one fixed point for the linear case of $C = 0$. By implementing the linear stability analysis, we find that only one of two fixed points for the nonlinear case is stable, marked by the solid lines (see Figs. 1(c) and 1(d)). In particular, we observe that the steady contrast α for the nonlinear case is larger than the one for the linear case. This means that the coherence can be enhanced by the combination of the dissipation and the nonlinearity. In addition, we find that the coherence may be enhanced by the imaginary coupling strength Λ, see Fig. 1(c). As Λ increases, the coherence slowly decreases at first and it then increases. This is similar to the dissipation-induced coherence in previous works.[54–56]

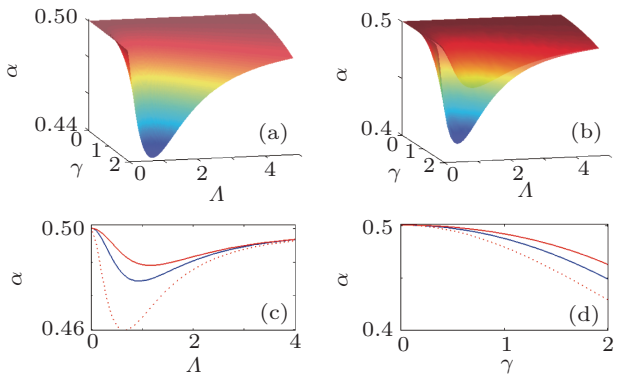


Fig. 1. (color online) Dependence of the steady contrast α on the relative dissipation strength γ and the imaginary coupling strength Λ. The nonlinearity C is chosen as (a) 0 and (b) 1. Panels (c) and (d) are sections of panels (a) and (b) for $\gamma = 1$ and $\Lambda = 1$, respectively. The red solid (dotted) lines correspond to the stable (unstable) steady states for the nonlinear case, and the blue solid lines are steady states for the linear case. The other parameters are given as $\Omega = 1$ and $\delta = 0$.

In Fig. 2, we show how the nonlinearity C affects the contrast α. For weak nonlinearity, the contrast α has two different values corresponding to one stable and one unstable fixed point. As the nonlinearity increases, a bifurcation appears at a certain critical value of the nonlinearity. This bifurcation of the contrast α is associated with the occurrence of one stable and one unstable point beyond the critical nonlinearity. Here, the red solid lines denotes the stable fixed points and the blue dotted lines represent the unstable fixed points.

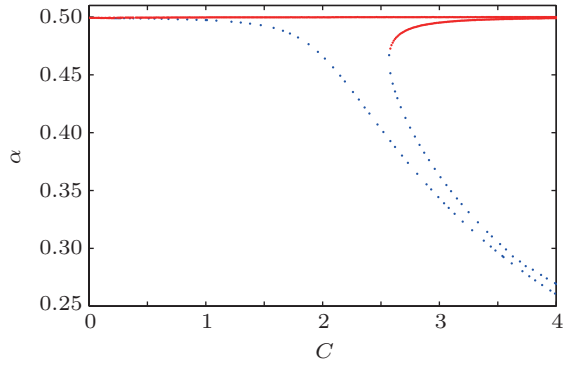


Fig. 2. (color online) The steady contrast α versus the nonlinearity C for $\Omega = 1$, $\gamma = 0.4$, and $\Lambda = 0.3$. Here the red solid lines correspond to the stable fixed points, and the blue dotted lines correspond to the unstable fixed points.

4. Nonlinear dissipative dynamics

Based upon our understanding of the steady states mentioned above, in this section, we analyze the mean-field dynamical behavior arising from the interplay of dissipation and nonlinearity. For the case that the dissipation strength in one of hyperfine levels is zero, that is, $\Lambda = 0$, the corresponding NH Hamiltonian is reduced to those in Refs. [49] and [50]. The mean-field dynamics has been studied in detail for this case, in which the dissipation enhanced self-trapping states have been revealed.[49,50] In this work, for simplicity, we focus on considering the following two cases: Case 1 $\gamma = 0$ and Case 2 $\gamma \neq 0$ and $\Lambda \neq 0$.

Case 1 $\gamma = 0$

Under the condition of $\Gamma_1 = \Gamma_2$, the relative dissipation between the two hyperfine levels vanishes; that is, $\gamma = 0$. Therefore, the mean-field Bloch equations are given as

$$\begin{aligned} \dot{s_x} &= -(\delta + 2Cs_z)s_y - \Lambda(1 - 4s_x^2)/2, \\ \dot{s_y} &= (\delta + 2Cs_z)s_x - 2\Omega s_z + 2\Lambda s_x s_y, \\ \dot{s_z} &= 2\Omega s_y + 2\Lambda s_z s_x, \end{aligned} \tag{14}$$

with the total probability n satisfying

$$\dot{n} = -\frac{\Lambda}{2}(2s_x + 1)n. \tag{15}$$

In Fig. 3, we show the dynamic behavior of the Bloch equation (14) on the Bloch sphere for the Hermitian case of $\Lambda = 0$ (top) and the NH case of $\Lambda = 0.4$ (bottom) with $\Omega = 1$ and $\delta = 0$. For the Hermitian case of $\Lambda = 0$, the Bloch vectors evolve periodically on the surface of the Bloch sphere and form closed orbits dependent upon initial conditions. There are two stable centers at $s_y = s_z = 0$ and $s_x = \pm 1/2$, which are shown in Fig. 3(a). When the nonlinearity strength C increases, one of the two centers becomes unstable and a saddle and two stable centers appear after a bifurcation, which are shown in Fig. 3(b). In the case of $\Lambda = 0.4$ (bottom), we see a drastic modification of these patterns. On the one hand, all orbits on the surface of the Bloch sphere become non-closed. On the other hand, the system starting from different initial states may relax to the same state of $s_y = s_z = 0$ and $s_x = -1/2$, see Figs. 3(c) and 3(d). Furthermore, the change of nonlinearity and dissipation only modifies the evolution paths and dissipation velocities to the final state. Therefore, in the case of $\gamma = 0$, for different nonlinearities and initial atom populations, the final state will be completely definite; that is, it is an equal population state.

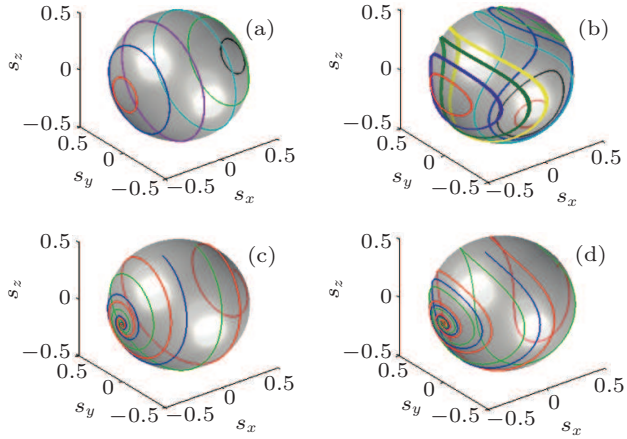


Fig. 3. (color online) Mean-field dynamics on the Bloch sphere for the Hermitian ($\Lambda = 0$, top) and NH ($\Lambda = 0.4$, bottom) cases for $\Omega = 1$, $\delta = 0$ and different values of the nonlinearity [$C = 0$ (left), 2 (right)]. Different tinctorial orbits on the Bloch sphere correspond to different initial conditions.

To better understand the mean-field dynamics, we analyze the fixed points and their stability. The fixed points are determined by

$$\begin{aligned} s_z^0 &= \frac{\Omega s_x^0 \delta}{\Omega^2 - 2C\Omega s_x^0 + \Lambda^2 (s_x^0)^2}, \\ (s_x^0)^2 &+ \frac{(s_x^0)^2 \delta^2 [\Omega^2 + \Lambda^2 (s_x^0)^2]}{[\Omega^2 - 2C\Omega s_x^0 + \Lambda^2 (s_x^0)^2)]^2} - \frac{1}{4} = 0. \end{aligned} \tag{16}$$

For the case of $\delta = 0$, we have two stationary states $s_x^0 = \pm 1/2$ and $s_y^0 = s_z^0 = 0$ from Eq. (14). However, considering Eq. (15) together, we only have one stable fixed point

$$s_k^0 = \begin{pmatrix} -1/2 \\ 0 \\ 0 \end{pmatrix}. \tag{17}$$

This explains why all initial states finally decay into this stable fixed point.

Case 2 $\gamma \neq 0$ and $\Lambda \neq 0$

Now, we consider the general case of $\gamma \neq 0$ and $\Lambda \neq 0$, which obeys the Bloch equations Eq. (6). In Fig. 4, we show the mean-field dynamics on the Bloch sphere for the two different cases: $\gamma > \Lambda$ (top) and $\gamma < \Lambda$ (bottom) with $\Omega = 1$ and $\delta = 0$. Similarly, the orbits on the surface of the Bloch sphere are not closed. In the case of $\gamma > \Lambda$, it is observed that, for linear and weakly nonlinear cases, all different initial states will always evolve into the same final state, as shown in Figs. 4(a) and 4(b). However, for strongly nonlinear cases, different initial states will evolve into different final states. As shown in

Fig. 4(c), for the case of $C = 5$, two different initial states evolve into different final states. Therefore, for $\gamma > \Lambda$, the change of the nonlinearity and initial states not only can modify the evolution paths and dissipation velocities to the final state but also may change the final state. However, for $\gamma < \Lambda$, independent of the initial state and nonlinearity strength, the system will always evolve to the same point on the Bloch sphere, which corresponds to the same final states, while the change of nonlinearity modifies its evolution path and dissipation velocity to the final state, as shown in Figs. 4(d)–4(f). After a further calculation, we find that for $\gamma > \Lambda$, the system has two stable fixed points, while $\gamma < \Lambda$, the system has only one stable fixed points. So the competition between γ and Λ results in different final states. It is important to note that the dissipation can be controlled by shining a laser beam onto the condensates[67] and relative dissipation rate γ can also be changed at the same time. Therefore, the combination of nonlinearity and dissipation can be used for controlling the dynamics.

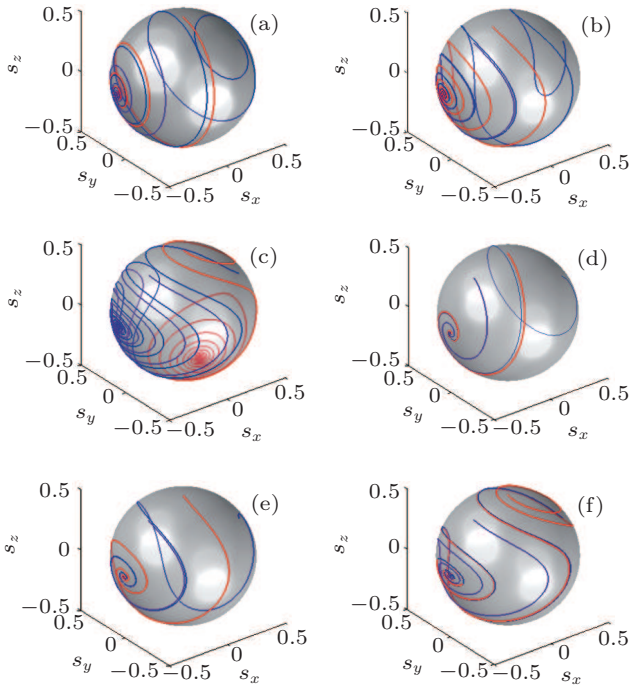


Fig. 4. (color online) Mean-field dynamics on the Bloch sphere for the case $\gamma > \Lambda$ ((a)–(c)) and $\gamma < \Lambda$ ((d)–(f)) for $\delta = 0$ and $\Omega = 1$. (a)–(c) $\gamma = 0.4$, $\Lambda = 0.15$; $C = 0.0$ (a), 1.5 (b), 5.0 (c). (d)–(f) $\gamma = 0.05$, $\Lambda = 0.324$; $C = 0.0$ (d), 1.5 (e), 5.0 (f). Here, different tinctorial orbits in the Bloch sphere correspond to different initial conditions with $s(0) = [0,0,0.5]$ (red), $[0.48,0,0.14]$ (blue), $[0.3,0,0.4]$ (purple).

Below, we discuss how to control the population switching by controlling the nonlinearity and dissipation. We assume that all of the atoms initially occupy the second hyperfine level, which can be easily prepared in labs.[6] This initial state corresponds to the north pole of the Bloch sphere. In Fig. 5, we show the time evolution of $s_z(t)$ for the case of $\gamma = 0$ with two different values of the nonlinearity. In this case, it is found that an initial self-trapped state can finally evolve into an equal-population state. In Fig. 6, we show the numerical results for $s_z(t)$ in the case of $\gamma > \Lambda$ with three different values of nonlinearity. From this numerical calculation, we find that the system may switch from an self-trapped state to another self-trapped state. The numerical data show that strong nonlinearity drives the system close to self-trapped state with large population imbalance, $s_z \approx -0.5$. In addition, for $\gamma < \Lambda$, the system will jump from an initial self-trapped state to an equal-population state, as illustrated in Fig. 7. The full many-particle result shows a very similar behavior. By varying the relative dissipation rate γ, one can observe the switching between different self-trapped states (see Fig. 6) or the switching from a self-trapped state to an equal-population state (see Figs. 5 and 7). On the contrary, one can also understand the dissipative mechanism of an open two-component BEC system by measuring the population difference between two hyperfine levels.

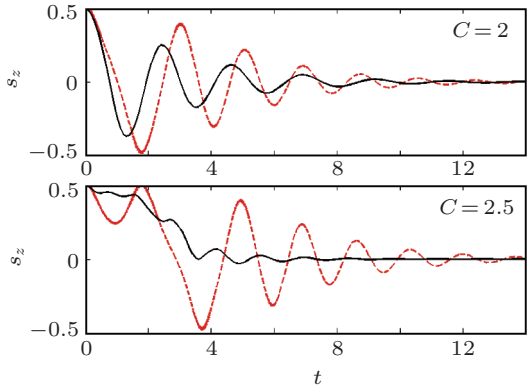


Fig. 5. (color online) Time evolution of $s_z(t)$ in the case of $\gamma = 0$ with $C = 2$ and $C = 2.5$. Here, $\delta = 0$, $\Omega = 1$, $\Lambda = 0.2$, $\Upsilon = 1$ and the initial state locates at the north pole. The dashed red lines and solid black lines correspond to mean-field and many-particle with $N = 10$ behavior, respectively.

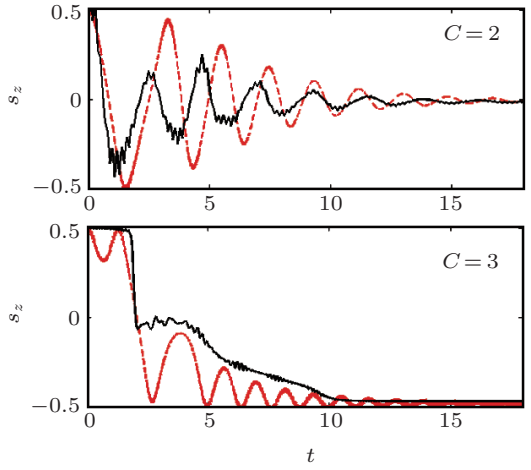


Fig. 6. (color online) Time evolution of $s_z(t)$ in the case of $\gamma > \Lambda$ with $C = 2$ and $C = 3$. Here, $\delta = 0$, $\Omega = 1$, $\gamma = 0.4$, $\Lambda = 0.15$, $\Upsilon = 1$ and the initial state locates at the north pole. The dashed red lines and solid black lines correspond to mean-field and many-particle with $N = 10$ behavior, respectively.

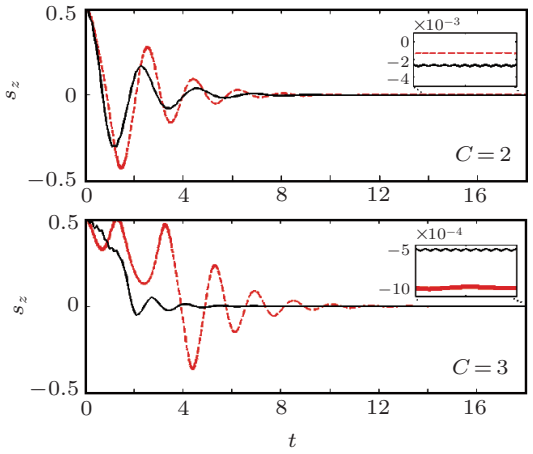


Fig. 7. (color online) Time evolution of $s_z(t)$ in the case of $\gamma < \Lambda$ with $C = 2$ and $C = 3$. Here, $\delta = 0$, $\Omega = 1$, $\gamma = 0.05$, $\Lambda = 0.324$, $\Upsilon = 1$ and the initial state locates at the north pole. The dashed red lines and solid black lines correspond to mean-field and many-particle with $N = 10$ dynamics, respectively. The inset gives the enlarged region between the two dotted lines.

5. Conclusions

In summary, we explore the many-body quantum coherence and population dynamics in a two-component condensate coupled with a continuum. The system is described by an NH Bose–Hubbard dimer whose diagonal and off-diagonal Hamiltonian elements are both complex numbers. The combination of dissipation and nonlinearity may induce different steady states and modify the bifurcation of coherence. By tuning the nonlinearity and dissipation, the coherence enhancement exhibits. In particular, different relative dissipation strengths between two hyperfine levels γ will drive the two-component condensate into different stable states. Under the condition of $\gamma = 0$, the atoms always evolve into a balanced state with equal population. In the case of $\gamma \neq 0$, dependent upon the values of γ and Λ, the system will evolve into different final states. For $\gamma > \Lambda$, the system always evolve into a steady state with self-trapping. The change of nonlinearity and initial state can not only modify the evolution path and the dissipation velocity to the final state but can also change the strength of self-trapping. For $\gamma < \Lambda$, the atoms always evolve to the same quasi-equal-population state with a small s_z in order of 10^{-3}, although the evolution path might be different for different nonlinearity strengths.

Our results show that the combination of dissipation and nonlinearity can be used to manipulate the steady behaviors; such as, controlling the transition between two self-trapped states or between a self-trapped state and a non-self-trapped state. Therefore, our results provide an alternative route for manipulating the many-body coherence and population dynamics by utilizing dissipation and nonlinearity.

With currently avaliable techniques, it is possible to realize our model in experiments. It has suggested that autoionizing Rydberg states[59,68] can be used as a continuum. In recent researches, the coupling between Bose–Einstein condensed atoms and highly excited Rydberg states have been reported.[69] Therefore, based on the experimental techniques for observing internal Josephson effects in a two-component condensate,[6] by coupling the condensed atoms to a continuum of autoionizing Rydberg states, our results may be tested in future experiments.

References

[1] Matthews M R, Hall D S, Jin D S, Ensher J R, Wieman C E, Cornell E A, Dalfovo F, Minniti C and Stringari S 1998 *Phys. Rev. Lett.* **81** 243
[2] Hall D S, Matthews M R, Ensher J R, Wieman C E and Cornell E A 1998 *Phys. Rev. Lett.* **81** 1539
[3] Hall D S, Matthews M R, Wieman C E and Cornell E A 1998 *Phys. Rev. Lett.* **81** 1543
[4] Lewandowski H J, Harber D M, Whitaker D L and Cornell E A 2002 *Phys. Rev. Lett.* **88** 070403
[5] Erhard M, Schmaljohann H, Kronjäger J, Bongs K and Sengstock K 2004 *Phys. Rev. A* **69** 032705
[6] Zibold T, Nicklas E, Gross C and Oberthaler M K 2010 *Phys. Rev. Lett.* **105** 204101
[7] Li S C, Fu L B, Duan W S and Liu J 2008 *Phys. Rev. A* **78** 063621
[8] Chien C C and Cooper F 2013 *Phys. Rev. A* **87** 045602
[9] Williams J, Walser R, Cooper J, Cornell E and Holland M 1999 *Phys. Rev. A* **59** R31
[10] Lee C, Hai W, Luo X, Shi L and Gao K 2003 *Phys. Rev. A* **68** 053614
[11] Öhberg P and Santos L 2001 *Phys. Rev. Lett.* **86** 2918
[12] Kasamatsu K and Tsubota M 2004 *Phys. Rev. Lett.* **93** 100402
[13] Lee C, Hai W, Shi L, Zhu X and Gao K 2001 *Phys. Rev. A* **64** 053604
[14] Yao S F, Li Q Y and Li Z D 2011 *Chin. Phys. B* **20** 110307
[15] Wen L, Liu W M, Cai Y, Zhang J M and Hu J 2012 *Phys. Rev. A* **85** 043602
[16] Li F, Shu W X, Luo H L and Ren Z Z 2007 *Chin. Phys.* **16** 650
[17] Lee C, Hai W, Shi L and Gao K 2004 *Phys. Rev. A* **69** 033611
[18] Cirac J I, Lewenstein M, Mølmer K and Zoller P 1998 *Phys. Rev. A* **57** 1208
[19] Saito H, Kawaguchi Y and Ueda M 2007 *Phys. Rev. A* **76** 043613
[20] Saito H, Kawaguchi Y and Ueda M 2009 *Phys. Rev. Lett.* **102** 230403
[21] Li S C and Duan W S 2009 *Chin. Phys. B* **18** 4177
[22] Ostrovskaya E A and Kivshar Y S 2004 *Phys. Rev. Lett.* **92** 180405
[23] Lee C, Huang J, Deng H, Dai H and Xu J 2012 *Front. Phys.* **7** 109
[24] Xie Q and Hai W 2006 *Eur. Phys. J. D* **39** 277
[25] Xie Q and Hai W 2005 *Eur. Phys. J. D* **33** 265
[26] Chen Z D, Liang J Q, Shen S Q and Xie W F 2004 *Phys. Rev. A* **69** 023611
[27] Zhang G F, Yin W, Liang J Q and Yan Q W 2004 *Chin. Phys.* **13** 988
[28] Lee C 2006 *Phys. Rev. Lett.* **97** 150402
[29] Ng H T and Chu S 2012 *Phys. Rev. A* **85** 023636
[30] Ng H T and Chu S 2011 *Phys. Rev. A* **84** 023629
[31] Wu Y and Yang X 2003 *Phys. Rev. A* **68** 013608
[32] Yang X and Wu Y 2009 *Commun. Theor. Phys.* **52** 244
[33] Lee C, Alexander T J and Kivshar Y S 2006 *Phys. Rev. Lett.* **97** 180408
[34] Micheli A, Jaksch D, Cirac J I and Zoller P 2003 *Phys. Rev. A* **67** 013607
[35] Lee C, Fu L B and Kivshar Y S 2008 *Europhys. Lett.* **81** 60006
[36] Kuang L M, Tong Z Y, Ouyang Z W and Zeng H S 1999 *Phys. Rev. A* **61** 013608
[37] Kuang L M and Ouyang Z W 2000 *Phys. Rev. A* **61** 023604
[38] Lee C 2009 *Phys. Rev. Lett.* **102** 070401
[39] Sadler L E, Higbie J M, Leslie S R, Vengalattore M and Stamper-Kurn D M 2006 *Nature* **443** 312
[40] Fedichev P O, Kagan Y, Shlyapnikov G V and Walraven J T M 1996 *Phys. Rev. Lett.* **77** 2913
[41] Donley E A, Claussen N R, Cornish S L, Roberts J L, Cornell E A and Wieman C E 2001 *Nature* **412** 295
[42] Pethick C J and Smith H 2001 *Bose–Einstein Condensation in Dilute Gases* (Cambridge: Cambridge University Press)
[43] Muruganandam P and Adhikari S K 2002 *Phys. Rev. A* **65** 043608
[44] Saito H and Ueda M 2002 *Phys. Rev. A* **65** 033624
[45] Graefe E M and Korsch H J 2006 *Czech. J. Phys.* **56** 1007

[46] Graefe E M, Höning M and Korsch H J 2010 *J. Phys. A: Math. Theor.* **43** 075306
[47] Kohler S and Sols F 2002 *Phys. Rev. Lett.* **89** 060403
[48] Graefe E M, Günther U, Korsch H J and Niederle A E 2008 *J. Phys. A: Math. Theor.* **41** 255206
[49] Graefe E M, Korsch H J and Niederle A E 2008 *Phys. Rev. Lett.* **101** 150408
[50] Graefe E M, Korsch H J and Niederle A E 2010 *Phys. Rev. A* **82** 013629
[51] Hiller M, Kottos T and Ossipov A 2006 *Phys. Rev. A* **73** 063625
[52] Zhong H, Hai W, Lu G and Li Z 2011 *Phys. Rev. A* **84** 013410
[53] Shchesnovich V S and Konotop V V 2010 *Phys. Rev. A* **81** 053611
[54] Witthaut D, Trimborn F and Wimberger S 2008 *Phys. Rev. Lett.* **101** 200402
[55] Witthaut D, Trimborn F and Wimberger S 2009 *Phys. Rev. A* **79** 033621
[56] Hao Y and Gu Q 2011 *Phys. Rev. A* **83** 043620
[57] Devdariani A Z, Ostrovskiĭ V N and Sebyakin Y N 1976 *Sov. Phys. JETP* **44** 477
[58] Makhmetov G E, Borisov A G, Teillet-Billy D and Gauyacq J P 1994 *Europhys. Lett.* **27** 247
[59] Fano U 1961 *Phys. Rev.* **124** 1866
[60] Anglin J 1997 *Phys. Rev. Lett.* **79** 6
[61] Cui B, Wang L C and Yi X X 2012 *Phys. Rev. A* **85** 013618
[62] Li P, Li R and Li L 2012 *Rom. Rep. Phys.* **64** 1271
[63] Luo X, Huang J, Zhong H, Qin X, Xie Q, Kivshar Y S and Lee C 2013 *Phys. Rev. Lett.* **110** 243902
[64] Chen C, Hu H, Lei L and Zeng X 2012 *Math. Numer. Sin.* **34** 3
[65] Xie Q 2007 *Phys. Rev. A* **76** 043622
[66] Anglin J R and Vardi A 2001 *Phys. Rev. A* **64** 013605
[67] Bloch I, Hänsch T W and Esslinger T 1999 *Phys. Rev. Lett.* **82** 3008
[68] Matthias E, Zoller P, Elliott D S, Piltch N D, Smith S J and Leuchs G 1983 *Phys. Rev. Lett.* **50** 1914
[69] Heidemann R, Raitzsch U, Bendkowsky V, Butscher B, Löw R and Pfau T 2008 *Phys. Rev. Lett.* **100** 033601